Aging-induced pseudouridine synthase 10 impairs hematopoietic stem cells

Yuqian Wang,[1*] Zhenzhen Zhang,[2*] Hanqing He,[1] Jinghui Song,[3] Yang Cui,[1] Yunan Chen,[4] Yuan Zhuang,[5] Xiaoting Zhang,[5] Mo Li,[6] Xinxiang Zhang,[4] Michael Q. Zhang,[2,7,8] Minglei Shi,[2] Chengqi Yi,[5] and Jianwei Wang[1]

[1]School of Pharmaceutical Sciences, Tsinghua University, Beijing, China; [2]School of Medicine, Tsinghua University, Beijing, China; [3]Department of Bioengineering, University of California San Diego, La Jolla, CA, USA; [4]Beijing National Laboratory for Molecular Sciences, Key Laboratory of Bioorganic Chemistry and Molecular Engineering of Ministry of Education, College of Chemistry and Molecular Engineering, Peking University, Beijing, China; [5]Department of Basic Medical Sciences, School of Medicine, Institute for Immunology, Beijing Key Laboratory for Immunological Research on Chronic Diseases, THU-PKU Center for Life Sciences, Tsinghua University, Beijing, China; [6]Center for Reproductive Medicine, Department of Obstetrics and Gynecology, Peking University Third Hospital, Beijing, China; [7]MOE Key Laboratory of Bioinformatics; Division and Center for Synthetic & Systems Biology, BNRist, Department of Automation, Tsinghua University, Beijing, China and [8]Department of Biological Sciences, Center for Systems Biology, the University of Texas, Richardson, TX, USA

**YW and ZZ contributed equally as first authors.*

Correspondence:
M.Q. Zhang
michael.zhang@utdallas.edu
M. Shi
shiml79@tsinghua.edu.cn
C. Yi
chengqi.yi@pku.edu.cn
J. Wang
jianweiwang@mail.tsinghua.edu.cn;
wangjianwei@ihcams.ac.cn

Received: October 4, 2022.
Accepted: May 4, 2023.
Early view: May 11, 2023.

https://doi.org/10.3324/haematol.2022.282211

Abstract

Aged hematopoietic stem cells (HSC) exhibit compromised reconstitution capacity and differentiation-bias towards myeloid lineage, however, the molecular mechanism behind it remains not fully understood. In this study, we observed that the expression of pseudouridine (Ψ) synthase 10 is increased in aged hematopoietic stem and progenitor cells (HSPC) and enforced protein of Ψ synthase 10 (PUS10) recapitulates the phenotype of aged HSC, which is not achieved by its Ψ synthase activity. Consistently, we observed no difference of transcribed RNA pseudouridylation profile between young and aged HSPC. No significant alteration of hematopoietic homeostasis and HSC function is observed in young *Pus10*$^{-/-}$ mice, while aged *Pus10*$^{-/-}$ mice exhibit mild alteration of hematopoietic homeostasis and HSC function. Moreover, we observed that PUS10 is ubiquitinated by E3 ubiquitin ligase CRL4^{DCAF1} complex and the increase of PUS10 in aged HSPC is due to aging-declined CRL4^{DCAF1}-mediated ubiquitination degradation signaling. Taken together, this study for the first time evaluated the role of PUS10 in HSC aging and function, and provided a novel insight into HSC rejuvenation and its clinical application.

Introduction

Hematopoietic stem cells (HSC) generate all of the blood cells throughout their life-span.[1,2] During aging, the function of HSC declines, featured as compromised reconstitution capacity and differentiation skewing towards myeloid lineage.[3,4] Although previous studies have identified various molecular signaling pathways promoting HSC aging,[5-8] the exact molecular mechanism is still not fully understood.

It has been known for several decades that more than 170 different types of chemical modifications to RNA exist.[9] Pseudouridine (Ψ), known as "the fifth nucleotide" in RNA, was first identified in 1951 and is the most abundant post-transcriptional RNA modification (with an estimated c/U ratio of 7–9%).[10-12] Ψ is generated from isomerization of uridine, which is catalyzed by Ψ synthases.[13-15] Ψ plays an important role in various aspects of RNA biology, and, therefore, participates in many biological process, including translational control,[16,17] RNA folding,[18-22] protein translation,[23-26] and clinical diseases.[27-32] A recent study revealed that dysfunction of PUS7 blocks the differentiation of HSC due to the lack of pseudouridylation of mTOG tRF.[16] Moreover, the expression of PUS7 is decreased in hematopoietic stem and progenitor cells (HSPC) of patients with myelodysplastic syndrome and delivery of pseudouridylated mTOG to HSPC of myelodysplastic syndromes patients improves their colony formation capacity and differentiation potential.[33] In addition, DKC1 is required for accurate HSC differentiation and maintenance of HSC function.[34,35] The above-mentioned studies reveal the importance of Ψ in modulating HSC differentiation and malignancies, however, whether Ψ participates in HSC aging has never been investigated.

In this study, we observed that the protein of Ψ synthase

10 (PUS10) is increased in aged HSPC. By conducting *in vivo* functional assay, we observed that enforced PUS10 impairs the reconstitution capacity of HSPC, which is independent of their Ψ synthase activity. By profiling the Ψ landscape in HSPC, we observed no difference in Ψ between young and aged HSPC at detectable locations. Moreover, we observed that PUS10 interacts with E3 ubiquitin ligase $CRL4^{DCAF1}$ complex and is ubiquitinated by this complex. Aging-declined $CRL4^{DCAF1}$ results in the accumulation of PUS10 in HSPC. Taken together, this study for the first time elucidated the role of PUS10 in HSC aging and function, and provided novel insights into HSC rejuvenation and its clinical application.

Methods

Mice

C57BL/6 mice (CD45.2), C57BL/6-SJL (CD45.1) mice were obtained from the Jackson Laboratory. *Pus10*$^{-/-}$ mice were kindly provided by Dr. Mo Li, Peking University Third Hospital, Beijing. *Pus10*$^{-/-}$ mice on C57BL/6N background were generated by deleting the 2nd exon using CRISPR-Cas9 system. The genomic RNA used to generate *Pus10*$^{-/-}$mice are listed in the *Online Supplementary Table S2*. The genotyping primers are listed in the *Online Supplementary Table S3*. The recipient mice (CD45.1/2) in the competitive transplantation assays were the first generation of C57BL/6 (CD45.2) and B6.SJL (CD45.1) mice. All mice were housed in specific pathogen-free conditions. All procedures were approved by the Institutional Animal Care and Use Committee (IACUC) of Tsinghua University.

Small RNA demethylase–pseudouridine-sequencing

Small RNA (<200 nt) was extracted and purified using miRNeasy Mini Kit (Qiagen) and RNeasy MinElute Cleanup Kit (Qiagen). Purified small RNA fragments were demethylated by wild-type and mutant AlkB, purified by phenol/chloroform extraction and ethanol precipitation, labeled by CMC. The demethylation reaction and CMC labeling were performed as described.[14] Briefly, 50 ng small RNA was denatured at 65°C for 5 minutes (min) and demethylated by wild-type and D135S mutant AlkB. The purified small RNA was denatured at 80°C for 5 min, added to BEU buffer with or without CMC, incubated at 37°C for 20 min, then purified by ethanol precipitation. The purified RNA was dissolved in sodium carbonate buffer and shaken at 37°C for 6 hours. The library was established as described.[14,36] Briefly, small RNA was dephosphorylated with CIP (NEB). The 3' adaptor ligation was added with T4 RNA ligase2, truncated KQ (NEB), followed by 5' Deadenylase (NEB) and RecJf (NEB) digestion. RNA was reverse transcribed by SuperScript III reverse transcriptase (Invitrogen), then digested by RNase H. The 5' adaptor ligation was added with T4 RNA ligase 1, high concentration (NEB). The ligated cDNA was amplified by Q5 High-Fidelity 2× Master Mix (NEB). The purified libraries were sequenced on Illumina NovaSeq 6000.

Identification of pseudouridine sites and levels on transcribed RNA

For transcribed RNA (tRNA) demethylase-pseudouridine sequencing (DM-Ψ-seq) data, the analysis was performed as described before.[14,36] Briefly, the adapter sequences of reads two were trimmed with Trim-galore v0.6.5 (parameters: -q 20--phred33--length 25-e 0.1--stringency 3). Polymerase chain recation (PCR) duplication was removed with Fastx_toolkit v0.0.14 before discarding the random barcode in the 5' end. Processed reads were further mapped to the genomic tRNA sequences from GtRNA database (http://gtrnadb.ucsc.edu/genomes/eukaryota/Mmusc10/) with Bowtie2 v2.3.5 (parameters: bowtie-a--best--strata--chunkmbs 2000). In order to identify the pseudouridine sites of tRNA, the following criteria were considered: i) the Ψ sites appearing in all independent replicates; ii) stop rate <1% in the BEU sample; iii) CMC coverage >50; iv) stop reads number >5 in the CMC sample; v) stop rate (CMC–BEU) difference >4%; vi) Fisher test adjusted *P* value <0.05. Finally, the Ψ level change for tRNA between young and old HSPC was evaluated and visualized via R package ggplot2.

Statistical analysis

Data are shown as mean ± standard deviation (SD). Student's *t* test (two-tailed unpaired) was used for comparisons between the groups using GraphPad Prism 6.0 software.

Results

PUS10 is increased in aged hematopoietic stem progenitor cells

Due to the scarcity of HSC, we purified HSPC by using the combination of $CD48^{-}LSK(cKit^{+}\ Sca1^{+}\ Lin^{-})$ according to previous reports.[37-39] The protein of PUS10 between young and aged HSPC was examined by western blot and it showed that PUS10 is increased upon aging (Figure 1A, B). In order to further confirm this result, we investigated the expression of PUS10 in a database, wherein the researchers compared the proteomic profile between young and aged HSC ($CD34^{-}CD150^{+}Flt3^{-}LSK$).[40] The result shows that PUS10 is indeed increased in aged HSC (Figure 1C).

Enforced PUS10 impairs the reconstitution capacity of hematopoietic stem and progenitor cells

In order to further investigate whether the increase of PUS10 plays a functional role on HSC, we cloned the cDNA of mouse *Pus10* into a lentiviral vector,[3] and it exhibited

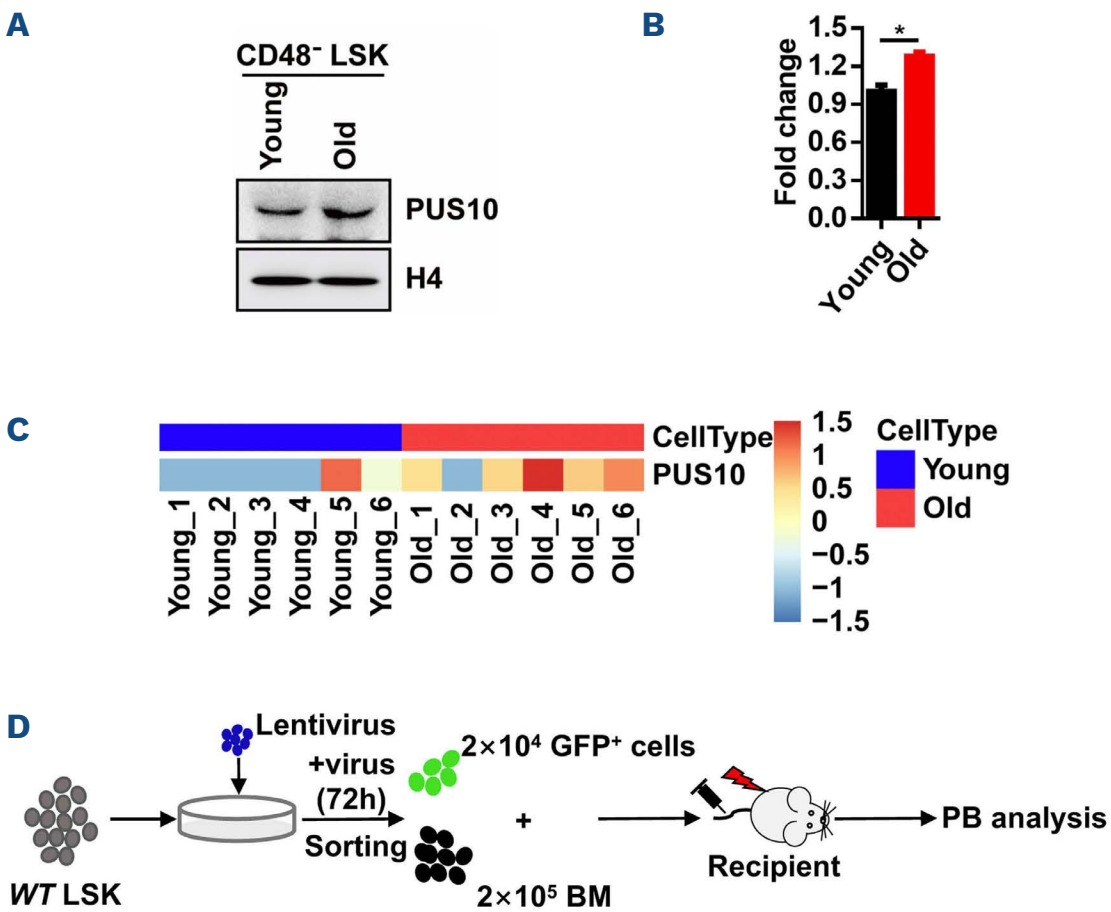

Continued on following page.

Figure 1. Aging-activated PUS10 impairs the reconstitution capacity of hematopoietic stem and progenitor cells independently on its enzymatic activity. (A) Representative western blot (WB) showing the expression of PUS10 in hematopoietic stem and progenitor cells (HSPC) between young (3-month-old) and aged (28-month-old) mice. (B) This histogram depicts the protein level of PUS10 in young and aged HSPC from quantitative WB data (N=2). (C) The protein expression of PUS10 in the proteomics dataset of young and old hematopoietic stem cells (HSC). (D) Experimental design of the transplantation assay. (E) These line plots depict the changes in peripheral blood (PB) chimerism in recipients transplanted with vector or PUS10-OE LSK (N=7 mice per group). (F) This histogram displays the lineage distribution of myeloid, T and B cells among donor-derived cells in the PB of vector and PUS10-OE recipients at the 12th week (N=7 mice per group). (G, H) Freshly isolated wild-type (WT) LSK cells were infected by PUS10-carrying lentivirus for 72 hours, and 50 green fluorescent protein-positive (GFP$^+$) HSPC (CD48$^-$ LSK) were sorted into 96-well plate and cultured in SFEM medium for 7 days. Then, the clones from vector or PUS10-OE HSPC were photographed and the cell numbers of these clones were analyzed. (G) These images show the expansion of vector or PUS10-OE HSPC.(H) The scatter plots show the cell numbers of these clones. (I) The result of liquid chromatography-tandem mass spectrometry shows the Ψ/U ratio in WT and *Pus10*$^{-/-}$ LK cells with overexpression of WT PUS10 or PUS10^{D342A}. (J) These line plots display the changes in PB chimerism in recipients transplanted with vector, PUS10-OE or PUS10^{D342A}-OE LSK (N=7-8 mice per group). All data are shown as mean ± standard deviation; **P*<0.05, ***P*<0.01, ****P*<0.001.

efficient overexpression of PUS10 (*Online Supplementary Figure S1A, B*). Freshly isolated WT LSK cells were infected by PUS10-carrying lentivirus; 72 hours later, 2×10^4 green fluorescent protein-positive (GFP$^+$) cells were purified and transplanted into lethally irradiated recipients together with 2×10^5 competitor cells (Figure 1D). Chimera in peripheral blood was evaluated every 4 weeks until the 12th week by using this gating strategy (*Online Supplementary Figure S1C, D*). The results showed that enforced PUS10 severely impairs the reconstitution capacity of HSPC (Figure 1E). Moreover, enforced PUS10 promotes HSPC differentiation bias towards the myeloid lineage (Figure 1F), which is a classical phenomenon of aged HSC. Consistently, enforced PUS10 significantly inhibits HSPC expansion *in vitro* (Figure 1G, H).

In order to investigate whether the inhibitory function of enforced PUS10 on HSPC depends on its Ψ catalytic activity, we mutated the key enzyme site of PUS10 to generate catalytic dead PUS10^{D342A} according to a previous study.[14] We first measured the Ψ/U ratio in WT and *Pus10*$^{-/-}$ lineage$^-$cKit^{+} (LK) cells using liquid chromatography-tandem mass spectrometry (LC-MS/MS). The result showed that targeted dysfunction of *Pus10* leads to a significant decrease of the Ψ/U ratio. In order to test whether PUS10^{D342A} is an inactive Ψ synthase, we reintroduced WT PUS10 and PUS10^{D342A} into *Pus10*$^{-/-}$ LK cells, and measured the Ψ/U ratio for them. The result showed that the decrease of the Ψ/U ratio upon *Pus10* deletion is rescued by the reintroduction of WT PUS10, but not PUS10^{D342A} (Figure 1I). This result indicates that the D342 residue is the key enzyme site for its Ψ synthase activity.

In order to investigate whether the Ψ synthase activity of PUS10 modulates HSC aging, freshly isolated WT LSK cells were infected with either PUS10 or PUS10^{D342A}-overexpressing lentivirus for 72 hours, and 2×10^4 GFP$^+$ cells were transplanted into lethally irradiated recipients together with 2×10^5 competitor cells. The chimera in peripheral blood was evaluated every 4 weeks until the 12th week. The results revealed that both enforced PUS10 and PUS10^{D342A} significantly impair the reconstitution capacity of HSPC (Figure 1J), indicating that the destructive role of PUS10 on HSPC is independent on its enzymatic activity.

No difference of pseudouridylation profile between young and aged hematopoietic stem and progenitor cells

We then set out to investigate whether aged HSC exhibit aberrant Ψ profile compared to young ones. Due to the limited cell number of HSC and the large amount of cells required for Ψ sequencing, we performed DM-Ψ-seq by using freshly isolated lineage$^-$ cells, which are hematopoietic stem and progenitor-enriched cells, from 3-month-old and 29-month-old mice according to an elegant approach[14,36] (Figure 2A). The result revealed no difference of the bulk Ψ profile between young and aged HSPC (Figure 2B). We then wondered whether the percentage of Ψ on certain sites of the tRNA exhibits a difference between them. In order to address this question, we evaluated all of the Ψ on detectable tRNA. The results revealed that the percentage of Ψ^{28}, Ψ^{32}, Ψ^{53} and Ψ^{54} of tRNA^{His}-GTG is static in young and aged HSPC (Figure 2C, D), and identical to other detected tRNA (*Online Supplementary Figure S2*). Briefly, these results indicate that not only the bulk Ψ profile but also the percentage of each Ψ on tRNA exhibits no difference between young and aged HSPC, which is consistent with the data that the toxicity of enforced PUS10 on HSPC is independent on its enzymatic activity.

Aging-declined CRL4^{DCAF1}-mediated ubiquitination degradation signaling leads to the increase of PUS10

Given that PUS10 is increased in aged HSPC and enforced PUS10 impairs the reconstitution capacity of HSPC, we then wondered how PUS10 is increased with aging. Firstly, we examined the mRNA level of *Pus10* in young and aged HSPC (CD48$^-$LSK) by reverse transcription PCR (RT-PCR), and the result revealed no difference of *Pus10* mRNA between them (Figure 3A). In order to confirm this observation, we examined the mRNA level of *Pus10* between young and aged HSC by exploring published RNA-sequencing data, and the result revealed that the mRNA level of *Pus10* remains static in young and aged HSC (*Online Supplemen-*

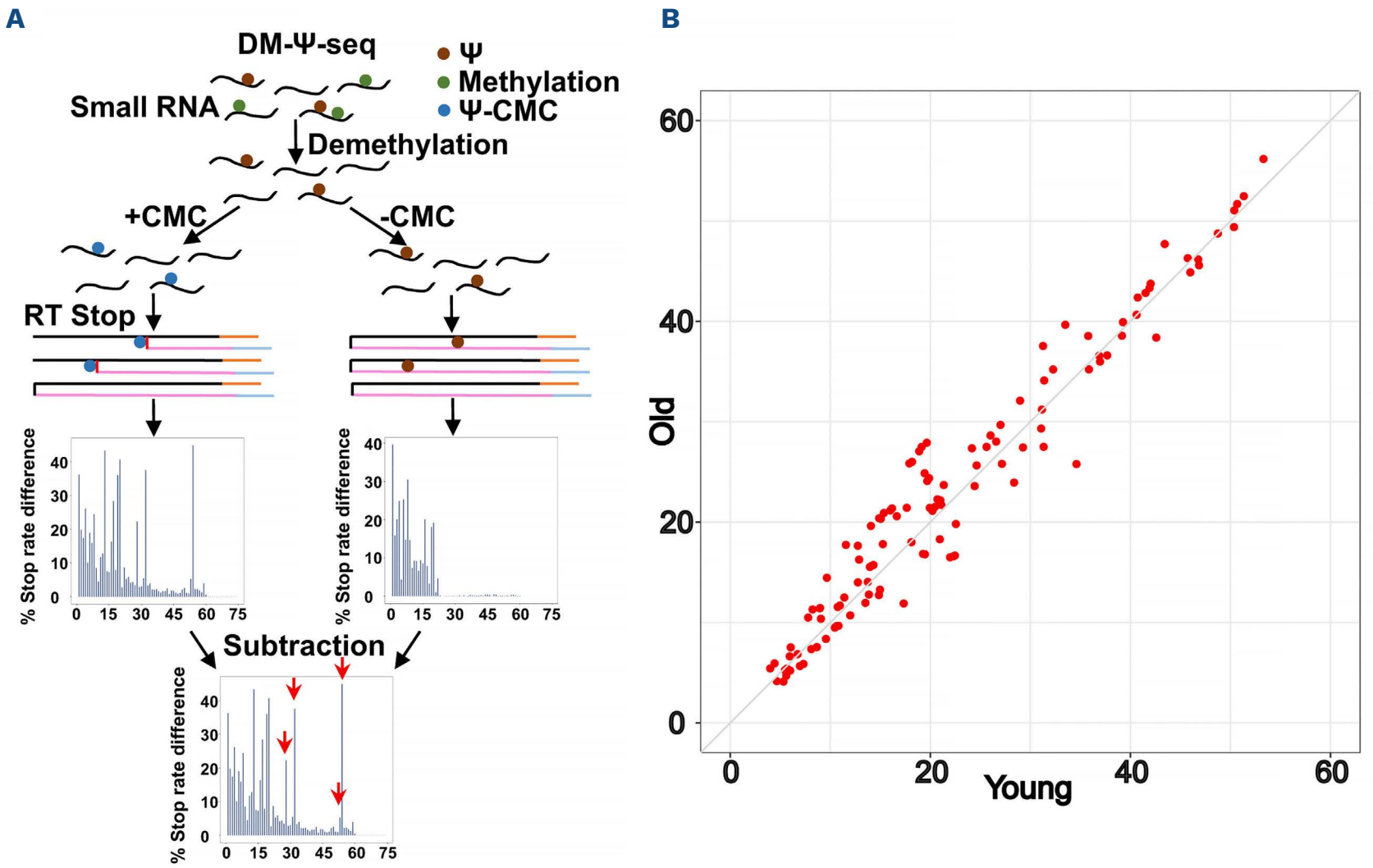

Figure 2. No difference of pseudouridine modification profile between young and aged hematopoietic stem and progenitor cells. (A-D) Lineage$^-$ cells were isolated from young (3-month-old) and aged (29-month-old) mice. Small RNA (<200 nt) was extracted and purified to perform demethylase-pseudouridine sequencing (DM–Ψ-seq). (A) Experimental design. (B) The scatter plot depicts Ψ levels in transcribed RNA (tRNA) between young and aged hematopoietic stem and progenitor cells (HSPC) (N=2). (C) Schematic of tRNA-His-GTG-2-1 shows Ψ sites Ψ^{28}, Ψ^{32}, Ψ^{53} and Ψ^{54}. (D) Ψ sites (red arrows) and levels of tRNA-His-GTG-2-1 are identified in young and aged HSPC. The x axis represents nucleotide position. The y axis represents Ψ levels.

A

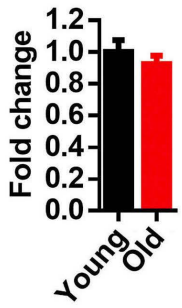

B

Protein	Unique Peptides
PUS10	3825
DDB1	3
DCAF1	2
CUL4B	1

C

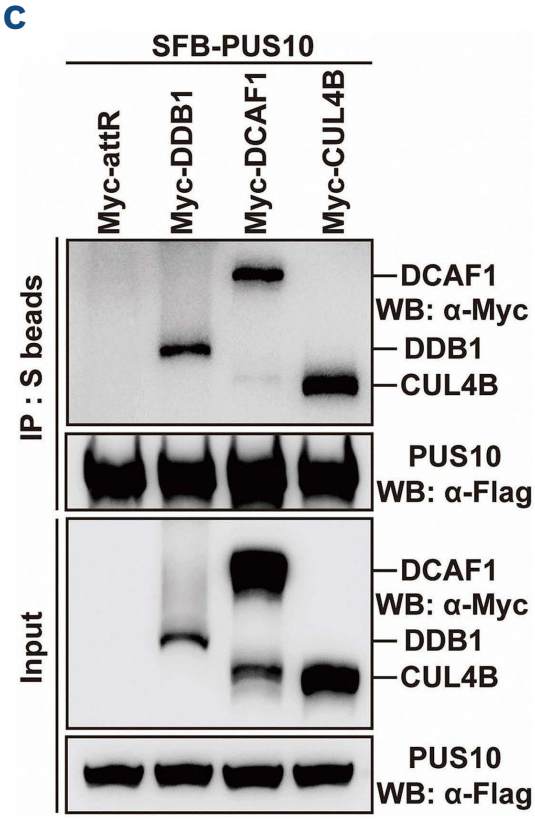

D

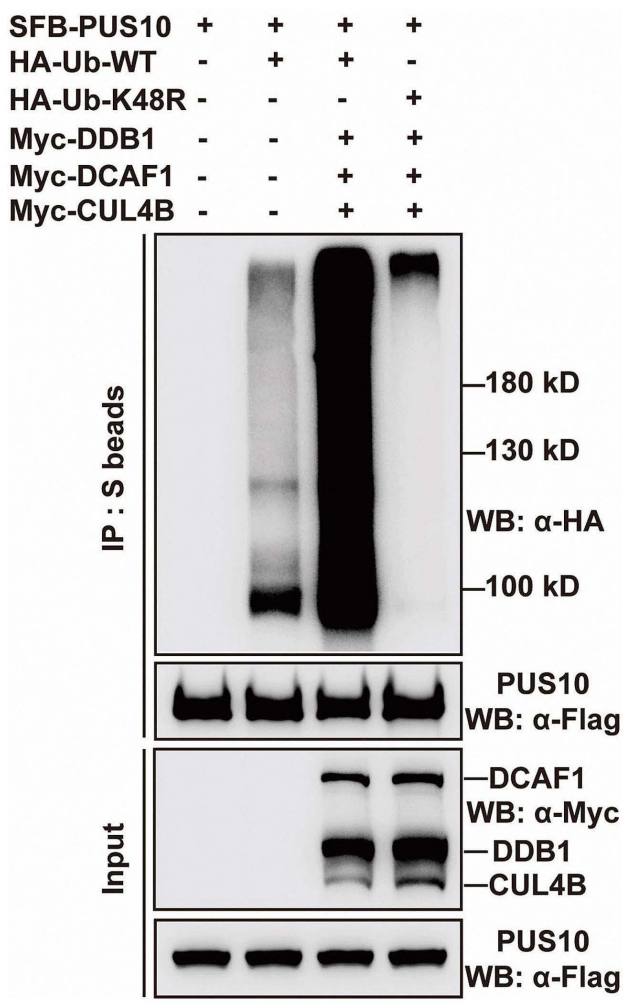

E

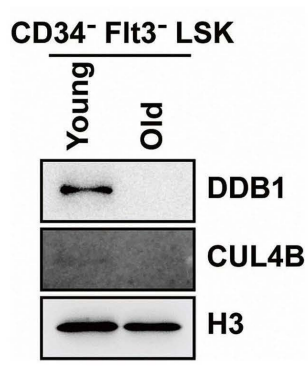

F

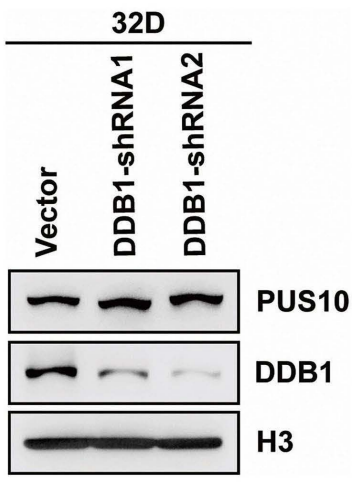

G

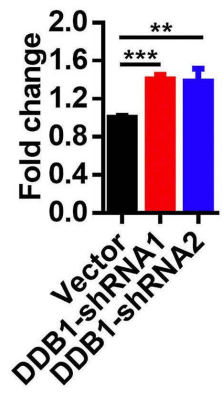

H

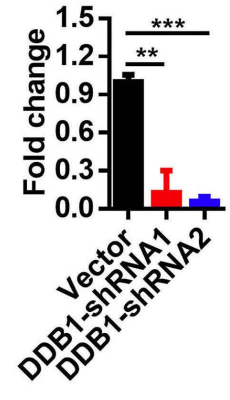

Figure 3. Aging-declined CRL4^{DCAF1}-mediated ubiquitination degradation signaling leads to the increase of PUS10. (A) This histogram depicts the mRNA expression of *Pus10* in young (2 months) and aged (31 months) hematopoietic stem and progenitor cells (HSPC). (B) Affinity purification of PUS10 protein from HEK293T cells stably expressing Flag-tagged PUS10. Proteins identified by mass spectrometry are listed. The bait protein is marked in bold letters. (C) HEK293T cells were co-transfected with plasmids encoding SFB-tagged PUS10 and Myc-tagged DDB1, DCAF1, CUL4B followed by co-immunoprecipitation using anti-Flag, anti-Myc antibody. Representative western blot (WB) shows that PUS10 interacts with DDB1, DCAF1 and CUL4B. (D) HEK293T cells were co-transfected with plasmids encoding SFB-tagged PUS10, Myc-tagged DDB1, DCAF1, CUL4B and HA-tagged Ub-WT or Ub-K48R followed by co-immunoprecipitation using anti-HA, anti-Flag, anti-Myc antibody. Representative WB shows that PUS10 is ubiquitinated by the CRL4^{DCAF1} complex. (E) Representative WB shows the expressions of DDB1 and CUL4B in young (3 months) and aged (28 months) HSPC. (F) 32D cells were infected by lentivirus carrying *Ddb1*-shRNA. 72 hours later, green fluorescent protein-positive (GFP$^+$) cells were sorted for WB to validate the expression of PUS10 and DDB1. Representative WB shows the expression of PUS10 and DDB1 in vector and DDB1-KD 32D cells. (G) This histogram depicts the protein level of PUS10 in vector and DDB1-KD 32D cells from quantitative WB data (N=2). (H) This histogram depicts the protein expression of DDB1 in vector and DDB1-KD 32D cells from quantitative WB data (N=3).

tary Figure S3). Then, it is conceivable that the increase of PUS10 might be modulated via post-transcriptional modification manner. In order to test this hypothesis, we purified proteins interacting with PUS10 via affinity purification and we observed that the $CRL4^{DCAF1}$ complex, including DDB1, DCAF1 and CUL4B, interacts with PUS10 (Figure 3B). $CRL4^{DCAF1}$ complex is E3 ubiquitin ligase targeting substrate for protein degradation.[41] In order to confirm this observation, we performed co-immunoprecipitation (Co-IP) assay by infecting HEK293T cells with S-protein, FLAG, and streptavidin-binding peptide (SFB)-tagged PUS10 together with Myc-tagged DDB1, DCAF1 or CUL4B respectively. Cell lysates were incubated with S-protein beads and probed with anti-Flag, anti-Myc antibodies. The result showed that PUS10 exhibits strong interaction with DDB1, DCAF1 and CUL4B (Figure 3C).

Previous study has shown that $CRL4^{DCAF1}$ complex participates in ubiquitin dependent degradation,[41] we then set out to determine whether $CRL4^{DCAF1}$ regulates PUS10 ubiquitination. Plasmids encoding SFB-tagged PUS10, Myc-tagged DDB1, DCAF1, CUL4B and HA-tagged wild-type ubiquitin (Ub-WT), mutant ubiquitin (Ub-K48R) were co-transfected into HEK293T cells; 24 hours later, cell lysates were collected to detect the ubiquitination of PUS10. The result revealed that $CRL4^{DCAF1}$ vigorously promotes the ubiquitination of PUS10 in cells expressing WT ubiquitin (Figure 3D). Compared with WT ubiquitin, the ubiquitination of PUS10 was completely abolished in cells expressing K48R ubiquitin, indicating that $CRL4^{DCAF1}$ promotes poly-ubiquitination of PUS10 via the formation of the K48 linkage.

Next, we set out to investigate whether the increase of PUS10 is due to the alteration of $CRL4^{DCAF1}$ in aged HSPC. We first evaluated the expression of $CRL4^{DCAF1}$ complex in young and aged HSPC. The result showed that the expression of DDB1 and CUL4B is decreased in aged HSPC (the expression level of DCAF1 is too low to be detected) (Figure 3E), which is negatively correlated with the alteration of PUS10 between young and aged HSPC (Figure 1A). Given that the protein level of PUS10, but not mRNA level, is elevated in aged HSPC (Figures 1A and 3A), and that PUS10 is poly-ubiquitinated by $CRL4^{DCAF1}$ complex (Figure 3D), and that DDB1 and CUL4B are decreased in aged HSPC (Figure 3E), we then wondered whether aging-declined $CRL4^{DCAF1}$ complex leads to the increase of PUS10. In order to test this hypothesis, we generated two efficient small hairpin RNA (shRNA) against *Ddb1* (Figure 3F, H; *Online Supplementary Table S2*), which is the key linker protein of $CRL4^{DCAF1}$ complex.[41] 32D cells were infected by s*hDdb1* carrying lentivirus for 72 hours, and GFP^+ cells were subjected to detect the protein level of PUS10 by western blot. The result showed that PUS10 is elevated upon the knockdown of *Ddb1* (Figure 3F, G).

Taken together, these data suggest that aging-declined $CRL4^{DCAF1}$-mediated ubiquitination degradation signaling leads to the accumulation of PUS10.

Young *Pus10*$^{-/-}$ mice exhibit no influence on hematopoietic homeostasis and hematopoietic stem cell function

The above-mentioned results revealed the functional role of *Pus10* in modulating HSC aging, we then wondered whether targeted dysfunction of *Pus10* plays a role in regulating hematopoietic homeostasis and HSC function. In order to address this question, we generated *Pus10* knockout (*Pus10*$^{-/-}$) mice on C57BL/6N background by deleting the 2nd exon using CRISPR-Cas9 system (Figure 4A, see details in the Material and Methods) and we achieved efficient deletion of PUS10 in LSK cells (Figure 4B, C).

We then performed complete blood count assay for *Pus10*$^{-/-}$ and age-matched control mice. The result revealed no difference of white blood cell (WBC), lymphocyte (LYM), neutrophil (NEUT), red blood cell (RBC) and platelet (PLT) count between *Pus10*$^{-/-}$ and WT mice (Figure 4D). We then sought to investigate the lineage composition in peripheral blood (PB) and bone marrow (BM) of *Pus10*$^{-/-}$ mice, including T cells, B cells and myeloid cells (*Online Supplementary Figure S4A*). The results revealed no difference of *Pus10*$^{-/-}$ mice compared to WT in PB (Figure 4E) and BM (Figure 4F).

We next analyzed HSPC of *Pus10*$^{-/-}$ mice, including common myeloid progenitors (CMP), granulocyte-macrophage progenitors (GMP), megakaryocyte-erythroid progenitors (MEP), common lymphoid progenitors (CLP), multipotent progenitor cells (MPP) and HSC (*Online Supplementary Figure S4B*). The results revealed no significant difference of the above-mentioned populations between *Pus10*$^{-/-}$ and WT mice (Figure 4G-K).

In order to further investigate the reconstitution capacity of *Pus10*$^{-/-}$ HSC, 20 freshly isolated *Pus10*$^{-/-}$ and WT HSC were transplanted into lethally irradiated recipients together with 3×10^5 competitor cells (Figure 5A). The chimera in the PB of recipients was evaluated every 4 weeks until the 16th week (*Online Supplementary Figure S4C, D*). The results showed that the reconstitution capacity of *Pus10*$^{-/-}$ HSC is comparable with WT ones (Figure 5B), while dysfunction of *Pus10* promotes the differentiation bias towards lymphoid lineage (34.31% *vs*. 48.43%; Figure 5C). Donor-derived HSC of recipients revealed no significant difference between *Pus10*$^{-/-}$ and WT mice (Figure 5D-F).

Aged *Pus10*$^{-/-}$ mice exhibit mild alteration of hematopoietic homeostasis and hematopoietic stem cell function

We then investigated the phenomenon of aged *Pus10*$^{-/-}$ mice. We performed complete blood count assay for aged WT and *Pus10*$^{-/-}$ mice (26-month-old). The result showed no significant difference of WBC, LYM, NEUT, RBC and PLT

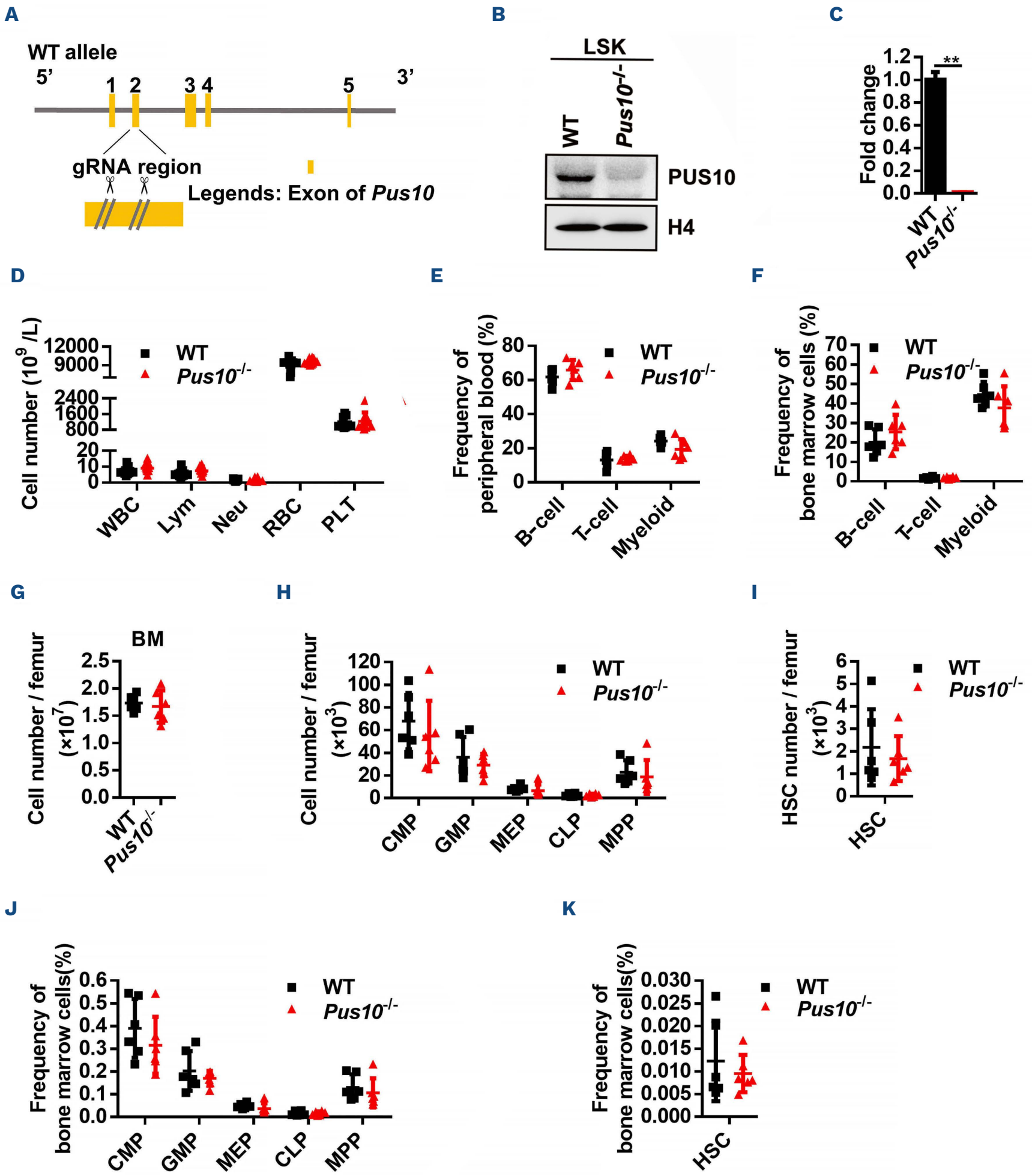

Figure 4. Young *Pus10*$^{-/-}$ mice exhibit no influence on hematopoietic homeostasis. (A) Schematic illustration of the *Pus10* knockout (*Pus10*$^{-/-}$) mice. (B) Representative western blot (WB) shows the expression of PUS10 in wild-type (WT) and *Pus10*$^{-/-}$ LSK cells. (C) This histogram depicts the protein expression of PUS10 in WT and *Pus10*$^{-/-}$ LSK cells from quantitative WB data (N=2). (D) The scatter plots show the numbers of white blood cells (WBC), lymphocytes (LYM), neutrophils (NEUT), red blood cells (RBC) and platelets (PLT) between WT and *Pus10*$^{-/-}$ mice. (E, F) The scatter plots depict the frequency of B cells, T cells and myeloid cells in peripheral blood (PB) (E) and bone marrow (BM) (F) of WT and *Pus10*$^{-/-}$ mice. (G) The scatter plots show the cell numbers of BM in WT and *Pus10*$^{-/-}$ femurs. (H-K) The scatter plots depict the cell numbers and frequency of common myeloid progenitors (CMP), granulocyte/macrophage progenitors (GMP), megakaryocytic/erythroid progenitors (MEP), common lymphoid progenitors (CLP), multipotent progenitor cells (MPP) and HSC in WT and *Pus10*$^{-/-}$ femurs. All data are shown as mean ± standard deviation; **P*<0.05, ***P*<0.01, ****P*<0.001.

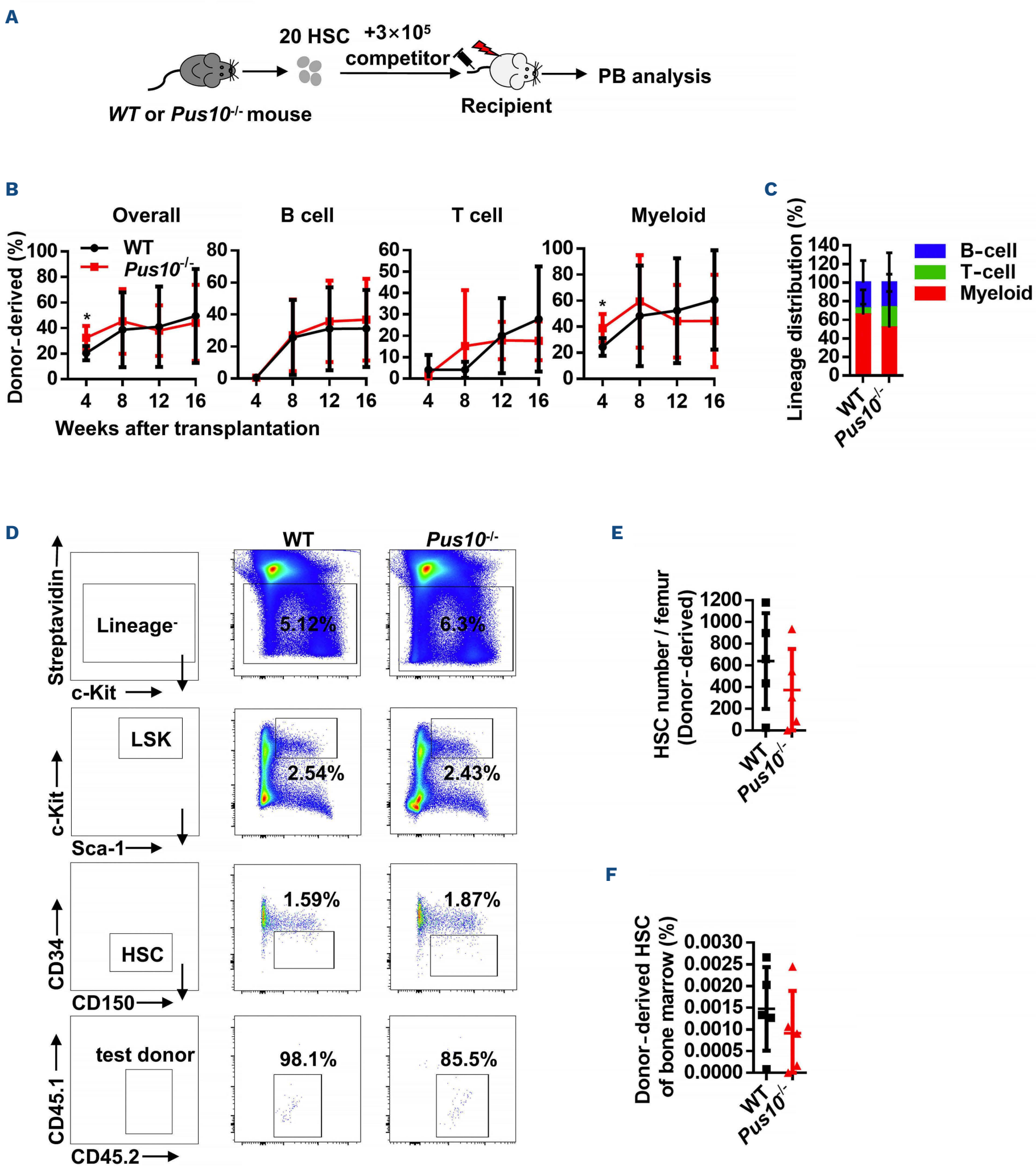

Figure 5. Young *Pus10*$^{-/-}$ mice exhibit no influence on hematopoietic stem cell function. (A) Experimental design of the competitive transplantation strategy. (B) These line plots depict the changes in peripheral blood (PB) chimerism in recipients transplanted with wild-type (WT) or *Pus10* knockout (*Pus10*$^{-/-}$) hematopoietic stem cells (HSC) (N=5 mice per group). (C) This histogram displays the lineage distribution of myeloid, T and B cells among donor-derived cells in PB of the recipients at the 16th week (N=5 mice per group). (D) The gating strategies for the frequency of the test donor-derived HSC. (E, F) The scatter plots depict the cell numbers (E) and frequency (F) of donor-derived HSC in recipients transplanted with WT or *Pus10*$^{-/-}$ HSC (N=5 mice per group). All data are shown as mean ± standard deviation; **P*<0.05, ***P*<0.01, ****P*<0.001.

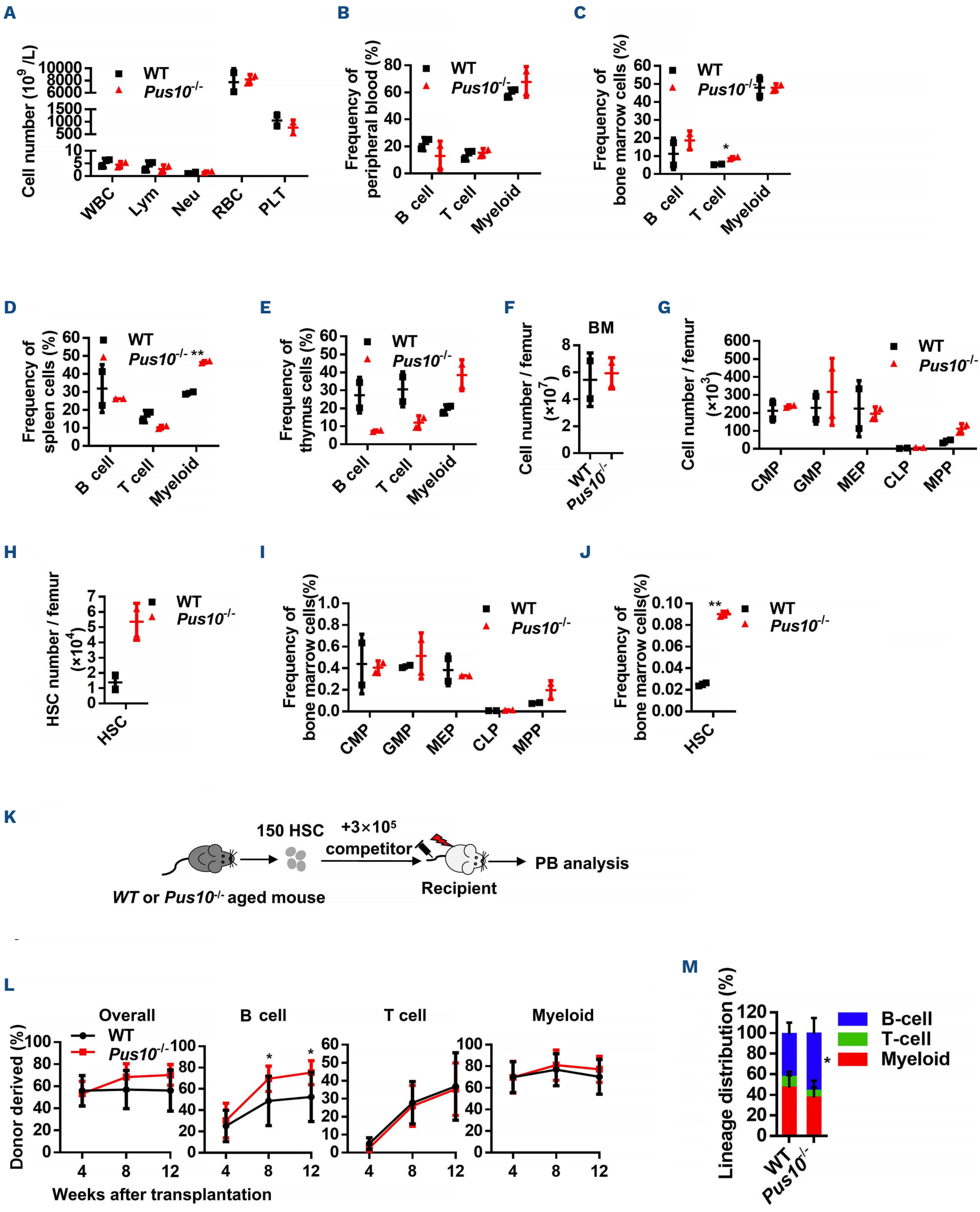

Continued on following page.

Figure 6. Aged *Pus10*$^{-/-}$ mice exhibit mild alteration of hematopoietic homeostasis and hematopoietic stem cell function. (A) The scatter plots show the numbers of white blood cells (WBC), lymphocytes (LYM), neutrophils (NEUT), red blood cells (RBC) and platelets (PLT) between aged wild-type (WT) and *Pus10* knockout (*Pus10*$^{-/-}$) mice. (B-E) The scatter plots depict the frequency of B cells, T cells and myeloid cells in the peripheral blood (PB) (B), bone marrow (C), spleen (D) and thymus (E) of aged WT and *Pus10*$^{-/-}$ mice. (F) The scatter plots show the cell numbers of bone marrow in WT and *Pus10*$^{-/-}$ femurs. (G-J) The scatter plots indicate the cell numbers and frequency of common myeloid progenitors (CMP), granulocyte/macrophage progenitors (GMP), megakaryocytic/erythroid progenitors (MEP), common lymphoid progenitors (CLP), multipotent progenitor cells (MPP) and hematopoietic stem cells (HSC) in WT and *Pus10*$^{-/-}$ femurs. (K) Experimental design of the transplantation assay. (L) These line plots depict the changes in PB chimerism in recipients transplanted with aged WT or *Pus10*$^{-/-}$ HSC (N=8-10 mice per group). (M) This histogram displays the lineage distribution of myeloid, T and B cells among donor-derived cells in the PB of the recipients at the 12th week (N=8-10 mice per group). All data are shown as mean ± standard deviation; **P*<0.05, ***P*<0.01, ****P*<0.001.

between aged WT and *Pus10*$^{-/-}$ mice (Figure 6A). We then analyzed the frequency of T cells, B cells and myeloid cells in PB, BM, spleen and thymus of aged *Pus10*$^{-/-}$ and WT mice. The results revealed no significant difference between them in the PB (Figure 6B) and thymus (Figure 6E). However, the percentage of T cells in the BM (Figure 6C) and the percentage of myeloid cells in the spleen (Figure 6D) of aged *Pus10*$^{-/-}$ mice are increased.

We next investigated HSPC of aged *Pus10*$^{-/-}$ and WT mice. The results indicated no significant difference of the CMP, GMP, MEP, CLP and MPP, while the frequency of HSC is increased in aged *Pus10*$^{-/-}$ mice compared to WT (Figure 6F-J). In order to further explore the reconstitution capacity of aged *Pus10*$^{-/-}$ HSC, 150 freshly isolated aged *Pus10*$^{-/-}$ and WT HSC were transplanted into lethally irradiated recipients together with 3×10^5 competitor cells (Figure 6K). The chimera in the PB of recipients was evaluated every 4 weeks until the 12th week. The results revealed that the reconstitution capacity of aged *Pus10*$^{-/-}$ HSC is comparable with WT ones, while dysfunction of *Pus10* promotes the differentiation bias towards B-cell lineage (Figure 6L, M).

In brief, our study for the first time revealed that enforced PUS10 impairs the reconstitution capacity of HSPC. Howerer, the hematopoietic homeostasis and reconstitution capacity of young *Pus10*$^{-/-}$ mice is comparable with control mice, while aged *Pus10*$^{-/-}$ mice exhibit mild alteration of hematopoietic homeostasis and HSC function. In summary, these data suggest that aging-diminished CRL4^{DCAF1}-mediated ubiquitination degradation signaling leads to the accumulation of PUS10, which impairs HSPC (Figure 7).

Discussion

Our study for the first time evaluated the role of PUS10 in HSC aging and function. This study will expand our understanding of RNA modification on HSC function regulation.

Post-transcriptional regulation in aged hematopoietic stem cells

An elegant study reported a proteomics resource from mass spectrometry of mouse young and aged HSC, and identified a subset of genes with apparent post-transcriptional alteration during aging.[40] This indicates that transcriptomic levels may not reflect the functional change of aged HSC. The alteration of the protein level achieved either by RNA or protein modification in aged HSC might play an essential role in promoting HSC aging. Our unpublished data confirmed this observation by identifying a group of RNA modification genes which modulate HSC aging. In addition, our study also identified that CRL4^{DCAF1}-mediated ubiquitination participated in regulating HSC aging by degrading PUS10 and other important proteins (*unpublished*). Whether there are other proteins modified by ubiquitination which lead to their changes during aging, thereby regulating HSC aging and other cell aging is a question worthy of study. It is also intriguing to investigate the molecular mechanism by which ubiquitin ligases are altered during aging.

Therefore, exploring the functional role of post-transcriptional modification (PTM) in aging might strengthen the understanding of aging on HSC and its clinical relevance.

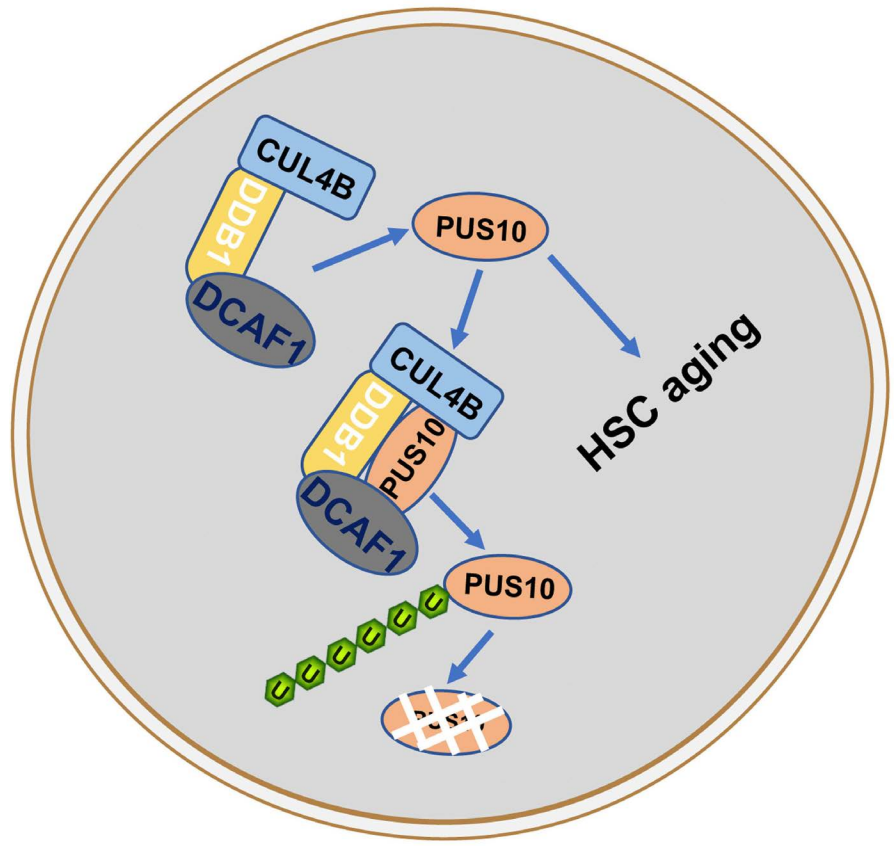

Figure 7. Aging-enforced PUS10 mediated by the decrease of ubiquitination degradation impairs hematopoietic stem and progenitor cells. The proposed model diagram illustrates the accumulation of PUS10 mediated by the decrease of ubiquitination degradation during aging impairs hematopoietic stem and progenitor cells (HSPC).

RNA epigenetics *versus* hematopoietic stem cell aging

In our study, we observed the Ψ profile is not changed in aged HSPC and the aging-increased PUS10 promotes HSC aging, which is not achieved by its Ψ synthase activity. Up to date, more than 170 RNA modifications have been identified and some of them play an essential role in various biological process and clinical diseases.[42,43] Whether other RNA modification profiles are altered in aged HSC and whether the corresponding enzymes are involved in regulating HSC aging is a question worthy of investigation. In this study, we performed Ψ profiling by using HSPC, but not pure HSC, due to the limitation of HSC number. Whether the Ψ profile of aged HSC is identical as we observed in HSPC is also a question worth investigating, which depends on the development of sequencing technology.

Disclosures

No conflicts of interest to disclose.

Contributions

JW and CY developed the concept. JW and CY developed the methodology. YW, ZZ, HH, JS, YC, YC, YZ and XZ carried out the investigation. JW, CY, MS, MQZ, XZ and ML performed the formal analysis. JW, CY, MS and MQZ provided resources. JW and CY wrote the manuscript. JW and CY acquired funding. JW, CY, MS and MQZ supervised the study.

Acknowledgments

We thank the Tsinghua-Peking Center for Life Sciences for facility and financial support.

Funding

This work was supported by grant numbers Z200022, 82250002, 81870118 and 2018YFA0800200 to JWW, and 2019YFA0110900, 2019YFA0802200 to CQY, and 81890991 to MS from the National Key R&D Program of China or the Beijing Municipal Science & Technology Commission and the National Natural Science Foundation of China.

Data-sharing statement

The data are available on request. All sequencing raw data were deposited in the National Center for Biotechnology Information Gene Expression Omnibus. The accession code is GSE213422 with the enter token atstusiqpxmhvmj.

References

1. Dzierzak E, Bigas A. Blood development: hematopoietic stem cell dependence and independence. Cell Stem Cell. 2018;22(5):639-651.
2. Morrison SJ, Scadden DT. The bone marrow niche for haematopoietic stem cells. Nature. 2014;505(7483):327-334.
3. He H, Xu P, Zhang X, et al. Aging-induced IL27Ra signaling impairs hematopoietic stem cells. Blood. 2020;136(2):183-198.
4. Dykstra B, Olthof S, Schreuder J, Ritsema M, de Haan G. Clonal analysis reveals multiple functional defects of aged murine hematopoietic stem cells. J Exp Med. 2011;208(13):2691-2703.
5. Wang J, Sun Q, Morita Y, et al. A differentiation checkpoint limits hematopoietic stem cell self-renewal in response to DNA damage. Cell. 2012;148(5):1001-1014.
6. Mohrin M, Shin J, Liu Y, et al. Stem cell aging. A mitochondrial UPR-mediated metabolic checkpoint regulates hematopoietic stem cell aging. Science. 2015;347(6228):1374-1377.
7. Norddahl GL, Pronk CJ, Wahlestedt M, et al. Accumulating mitochondrial DNA mutations drive premature hematopoietic aging phenotypes distinct from physiological stem cell aging. Cell Stem Cell. 2011;8(5):499-510.
8. Sun D, Luo M, Jeong M, et al. Epigenomic profiling of young and aged HSCs reveals concerted changes during aging that reinforce self-renewal. Cell Stem Cell. 2014;14(5):673-688.
9. Boccaletto P, Stefaniak F, Ray A, et al. MODOMICS: a database of RNA modification pathways. 2021 update. Nucleic Acids Res. 2022;50(D1):D231-D235.
10. Cohn WE, Volkin E. Nucleoside-5′-phosphates from ribonucleic acid. Nature. 1951;167(4247):483-484.
11. Charette M, Gray MW. Pseudouridine in RNA: what, where, how, and why. IUBMB Life. 2000;49(5):341-351.
12. Ge J, Yu YT. RNA pseudouridylation: new insights into an old modification. Trends Biochem Sci. 2013;38(4):210-218.
13. Spenkuch F, Motorin Y, Helm M. Pseudouridine: still mysterious, but never a fake (uridine)! RNA Biol. 2014;11(12):1540-1554.
14. Song J, Zhuang Y, Zhu C, et al. Differential roles of human PUS10 in miRNA processing and tRNA pseudouridylation. Nat Chem Biol. 2019;16(2):160-169.
15. Li X, Zhu P, Ma S, et al. Chemical pulldown reveals dynamic pseudouridylation of the mammalian transcriptome. Nat Chem Biol. 2015;11(8):592-597.
16. Guzzi N, Cieśla M, Ngoc PCT, et al. Pseudouridylation of tRNA-derived fragments steers translational control in stem cells. Cell. 2018;173(5):1204-1216.
17. Levi O, Arava YS. Pseudouridine-mediated translation control of mRNA by methionine aminoacyl tRNA synthetase. Nucleic Acids Res. 2021;49(1):432-443.
18. Bernick DL, Dennis PP, Hochsmann M, Lowe TM. Discovery of Pyrobaculum small RNA families with atypical pseudouridine guide RNA features. RNA. 2012;18(3):402-411.
19. Ni J, Tien AL, Fournier MJ. Small nucleolar RNAs direct site-specific synthesis of pseudouridine in ribosomal RNA. Cell. 1997;89(4):565-573.
20. Keffer-Wilkes LC, Veerareddygari GR, Kothe U. RNA modification enzyme TruB is a tRNA chaperone. Proc Natl Acad Sci U S A. 2016;113(50):14306-14311.
21. Leppik M, Liiv A, Remme J. Random pseuoduridylation in vivo reveals critical region of Escherichia coli 23S rRNA for ribosome assembly. Nucleic Acids Res. 2017;45(10):6098-6108.
22. Zhao X, Patton JR, Davis SL, Florence B, Ames SJ, Spanjaard RA. Regulation of nuclear receptor activity by a pseudouridine synthase through posttranscriptional modification of steroid receptor RNA activator. Mol Cell. 2004;15(4):549-558.
23. Anderson BR, Muramatsu H, Nallagatla SR. Incorporation of pseudouridine into mRNA enhances translation by diminishing PKR activation. Nucleic Acids Res. 2010; 38(17):5884-5892.
24. Kariko K, Muramatsu H, Welsh FA, et al. Incorporation of

pseudouridine into mRNA yields superior nonimmunogenic vector with increased translational capacity and biological stability. Mol Ther. 2008;16(11):1833-1840.
25. Svitkin YV, Cheng YM, Chakraborty T, Presnyak V, John M, Sonenberg N. N1-methyl-pseudouridine in mRNA enhances translation through eIF2alpha-dependent and independent mechanisms by increasing ribosome density. Nucleic Acids Res. 2017;45(10):6023-6036.
26. Borchardt EK, Martinez NM, Gilbert WV. Regulation and function of RNA pseudouridylation in human cells. Annu Rev Genet. 2020;54:309-336.
27. Bykhovskaya Y, Casas K, Mengesha E, Inbal A, Fischel-Ghodsian N. Missense mutation in pseudouridine synthase 1 (PUS1) causes mitochondrial myopathy and sideroblastic anemia (MLASA). Am J Hum Genet. 2004;74(6):1303-1308.
28. Shaheen R, Han L, Faqeih E, et al. A homozygous truncating mutation in PUS3 expands the role of tRNA modification in normal cognition. Hum Genet. 2016;135(7):707-713.
29. Festen EA, Goyette P, Green T, et al. A meta-analysis of genome-wide association scans identifies IL18RAP, PTPN2, TAGAP, and PUS10 as shared risk loci for Crohn's disease and celiac disease. PLoS Genet. 2011;7(1):e1001283.
30. de Brouwer APM, Abou Jamra R, Körtel N, et al. Variants in PUS7 cause intellectual disability with speech delay, microcephaly, short stature, and aggressive behavior. Am J Hum Genet. 2018;103(6):1045-1052.
31. Darvish H, Azcona LJ, Alehabib E, et al. A novel PUS7 mutation causes intellectual disability with autistic and aggressive behaviors. Neurol Genet. 2019;5(5):e356.
32. Arroyo JD, Jourdain AA, Calvo SE, et al. A genome-wide CRISPR death screen identifies genes essential for oxidative phosphorylation. Cell Metab. 2016;24(6):875-885.
33. Guzzi N, Muthukumar S, Ciesla M, et al. Pseudouridine-modified tRNA fragments repress aberrant protein synthesis and predict leukaemic progression in myelodysplastic syndrome. Nat Cell Biol. 2022;24(3):299-306.
34. Bellodi C, McMahon M, Contreras A, et al. H/ACA small RNA dysfunctions in disease reveal key roles for noncoding RNA modifications in hematopoietic stem cell differentiation. Cell Rep. 2013;3(5):1493-1502.
35. Gu BW, Fan JM, Bessler M, Mason PJ. Accelerated hematopoietic stem cell aging in a mouse model of dyskeratosis congenita responds to antioxidant treatment. Aging Cell. 2011;10(2):338-348.
36. Cui Q, Yin K, Zhang X, et al. Targeting PUS7 suppresses tRNA pseudouridylation and glioblastoma tumorigenesis. Nat Cancer. 2021;2(9):932-949.
37. Termini CM, Pang A. Syndecan-2 enriches for hematopoietic stem cells and regulates stem cell repopulating capacity. Blood. 2022;139(2):188-204.
38. Akinduro O, Weber TS, Ang H, et al. Proliferation dynamics of acute myeloid leukaemia and haematopoietic progenitors competing for bone marrow space. Nat Commun. 2018;9(1):519.
39. Tadokoro Y, Hoshii T, Yamazaki S, et al. Spred1 safeguards hematopoietic homeostasis against diet-induced systemic stress. Cell Stem Cell. 2018;22(5):713-725.
40. Zaro BW, Noh JJ, Mascetti VL, et al. Proteomic analysis of young and old mouse hematopoietic stem cells and their progenitors reveals post-transcriptional regulation in stem cells. eLife. 2020;9:e62210.
41. Jackson S, Xiong Y. CRL4s: the CUL4-RING E3 ubiquitin ligases. Trends Biochem Sci. 2009;34(11):562-570.
42. Shi H, Chai P, Jia R, Fan X. Novel insight into the regulatory roles of diverse RNA modifications: re-defining the bridge between transcription and translation. Mol Cancer. 2020;19(1):78.
43. Delaunay S, Frye M. RNA modifications regulating cell fate in cancer. Nat Cell Biol. 2019;21(5):552-559.